

Melittin–Phospholipase A₂ Synergism Is Mediated by Liquid–Liquid Miscibility Phase Transition in Giant Unilamellar Vesicles

Sein Min, Cyrus Picou, Hye Jin Jeong, Adam Bower, Keunhong Jeong, and Jean K. Chung*



Cite This: *Langmuir* 2024, 40, 7456–7462



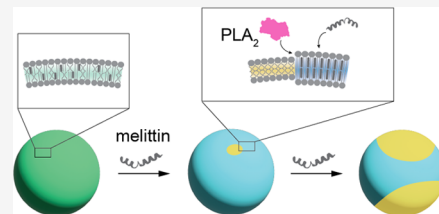
Read Online

ACCESS |

Metrics & More

Article Recommendations

ABSTRACT: The primary constituents of honeybee venom, melittin and phospholipase A₂ (PLA₂), display toxin synergism in which the PLA₂ activity is significantly enhanced by the presence of melittin. It has been shown previously that this is accomplished by the disruption in lipid packing, which allows PLA₂ to become processive on the membrane surface. In this work, we show that melittin is capable of driving miscibility phase transition in giant unilamellar vesicles (GUVs) and that it raises the miscibility transition temperature (T_{misc}) in a concentration-dependent manner. The induced phase separation enhances the processivity of PLA₂, particularly at its boundaries, where a substantial difference in domain thickness creates a membrane discontinuity. The catalytic action of PLA₂, in response, induces changes in the membrane, rendering it more conducive to melittin binding. This, in turn, facilitates further lipid phase separation and eventual vesicle lysis. Overall, our results show that melittin has powerful membrane-altering capabilities that activate PLA₂ in various membrane contexts. More broadly, they exemplify how this biochemical system actively modulates and capitalizes on the spatial distribution of membrane lipids to efficiently achieve its objectives.



INTRODUCTION

Rich heterogeneity is a hallmark of living cell membranes.¹ In particular, macroscopic liquid–liquid miscibility phase transition observed in model vesicles systems has been associated with heterogeneity in cells, even though it is clear that functional plasma membrane domains are considerably more complicated.^{2,3} Nevertheless, there is evidence that cell membranes are poised near a miscibility phase transition,⁴ and a growing body of studies suggest that cells can tune the outcome of biochemical reactions by tipping the balance in lipid phase separation.^{5–8}

In this work, we investigated how the two principal components of bee venom, melittin and phospholipase A₂ (PLA₂), exploit the spatial distribution of lipids by triggering the liquid–liquid miscibility transition. Melittin is a 26-mer cationic, amphiphilic-membrane-active peptide classified as an antimicrobial peptide.^{9,10} Its binding to the membrane is a multistep process including electrostatic attraction to the membrane via anionic lipids, structural changes, and insertion to the membrane.¹¹ While the details of the exact mechanism by which melittin operates appears diverse and context-dependent, it generally brings about lysis of cell membranes by the formation of toroidal pores and detergent-like dissolution.^{9,12–16} The bee venom secretory PLA₂ is a 14 kDa enzyme that catalyzes the hydrolysis of a fatty acid chain in the *sn*-2 acyl position of a phospholipid, degrading the overall membrane.^{17,18}

Individually, both melittin and PLA₂ can cause cell lysis. However, lysis occurs to significantly greater extents in combination, and this synergistic effect has been observed in

both *in vitro* vesicles and live cells.^{19–22} In our previous work in solid-supported lipid bilayers using single-molecule tracking, we found that melittin deforms the membrane into island-like structures, and PLA₂ becomes processive at the edge of those structures and shows 25-fold higher apparent activity.²³ These results are consistent with the established notions that melittin disrupts the membrane structure, and PLA₂ becomes active at membrane defects.^{24,25}

Our findings in giant unilamellar vesicles (GUVs) with the capacity for phase transition reveal an additional dimension of the collaborative effects of melittin and PLA₂. GUVs composed of ternary composition (e.g., saturated phospholipids, unsaturated phospholipids, and cholesterol) have a capacity to undergo a temperature-dependent liquid–liquid demixing into liquid ordered (L_o) and liquid disordered (L_d) domains.²⁶ These systems have been used extensively to model the heterogeneous spatial distribution of cell membrane lipids.²⁷ The introduction of melittin into GUVs induces a shift in the miscibility transition equilibrium, favoring phase separation. This rearrangement causes the segregation of unsaturated and saturated lipids into distinct domains, creating a discontinuity in the lipid packing. PLA₂ lingers on the membrane at this

Received: December 18, 2023

Revised: March 20, 2024

Accepted: March 20, 2024

Published: March 28, 2024



membrane defect site and becomes processively catalytic. The alterations in the material properties of the membrane induced by PLA₂ make it more susceptible to melittin, leading to further phase separation and eventual lysis. The cumulative result is an exceptionally efficient lytic action, underscoring the intricate and synergistic impact of melittin and PLA₂ on membrane dynamics.

RESULTS AND DISCUSSION

Melittin Induces Lipid Phase Separation in GUVs. Our investigation focused on understanding how melittin and PLA₂ influence membrane phase separation behavior and lysis. To do this, we utilized giant unilamellar vesicles (GUVs) based on a well-characterized ternary mixture of DOPC, DPPC, and cholesterol. This mixture is known for its ability to undergo liquid–liquid demixing, providing a suitable model for studying these processes.² A small amount (0.1%) of Texas Red-DHPE (TR) and Oregon Green-DPHE (OG) were used as markers of the L_d and L_o phases, as they preferentially partition to the respective domains.⁵ This study employed two GUV compositions, GUV1 and GUV2, depending on the context of the experiment. GUV1 has a miscibility transition temperature (T_{misc}) below room temperature, while GUV2 exhibits a T_{misc} above room temperature. The compositions were 0.4:0.1:0.2:0.3 and 0.3:0.1:0.4:0.2 for DOPC:DOPS:DPPC:cholesterol for GUV1 and GUV2, respectively.

10% DOPS was included to facilitate melittin binding to the GUV membranes via the electrostatic interactions between the cationic melittin and anionic headgroup.²⁸ However, electrostatics play a minor role in overall membrane binding. Thermodynamically, melittin binding is almost exclusively driven by the hydrophobic effect where the amphiphilicity of the helical structure maintains melittin in the membrane.¹¹ Indeed, anionic lipids are not critical to melittin binding to membranes, and it has been shown to insert to neutral membranes.²⁹ The addition of charged lipids lowers T_{misc} .^{30–33} For example, GUVs composed of 0.4:0.4:0.2 DOPC:DPPC:cholesterol display T_{misc} of 37 °C, but when 10% DOPC is replaced by DOPS (GUV2), the T_{misc} is lowered to 28 °C. Similarly, the T_{misc} of GUV1 is expected to be significantly lower compared to the analogous ternary composition of 0.4:0.1:0.2:0.3 DOPC:DPPC:cholesterol ($T_{\text{misc}} = 19$ °C). Other than this, however, there was no qualitative deviation from expected biphasic temperature dependence, consistent with previous findings that charged lipids have minimal effect on the miscibility transition of the ternary GUV compositions.³³ Moreover, there have been works that examined lipid phase separation behavior using GUVs containing charged lipids without complications.^{5,34} Therefore, we conclude that DOPS does not obfuscate interpretation of the data.

First, the effect of melittin was examined on GUV1, which is homogeneous at room temperature (21 °C; Figure 1A), as a function of its concentration in the range 0.5–15 μM. Using GUV1 allowed the experiment to be carried out at room temperature. When melittin is added, phase separation occurs, showing a distinct separation of the L_d (TR fluorescence, yellow) and L_o (OG fluorescence, cyan) regions (Figure 1B). The probability of phase separation increased with rising melittin concentrations over the 0–10 μM range. The vesicles were lysed as the melittin concentration is further increased, and all vesicles are ruptured at an excess melittin concentration of 15 μM (Figure 1C). The melittin-dependent phase separation and lysis are shown in Figure 1D. These results

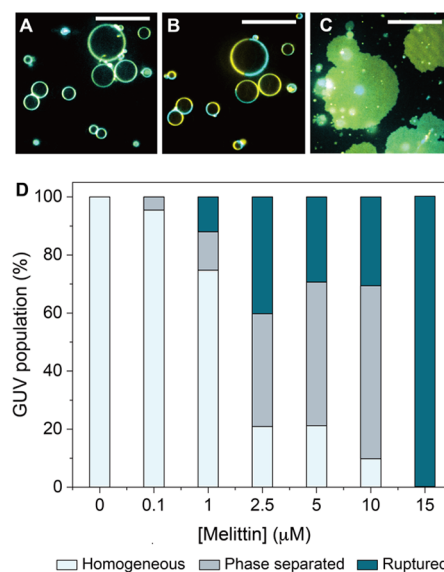


Figure 1. Confocal microscopy images of (A) a homogeneous GUV1 population at 0 μM melittin, (B) phase separated at 5 μM melittin, and (C) ruptured at 15 μM melittin. Scale bars: 20 μm. (D) The population of GUVs ruptured, phase separated, and homogeneous at varying melittin concentrations. Increasing the melittin concentration increased the population of GUVs that were phase separated and ruptured. Approximately 100 GUVs were analyzed at each concentration at room temperature, 21 °C.

suggest that the vesicles can accept melittin incorporation up to a point and accommodate phase separation, but a critical amount of melittin in the membrane causes lysis.

The observed facilitation of phase separation suggests that melittin raises the T_{misc} of the vesicles as it is incorporated into the membrane. Temperature-dependent experiments were performed on GUV2. GUV2 are homogeneous at room temperature, and we were able to observe increasing concentration of melittin inducing phase separation at increasing temperature. A population of ~100 GUVs were analyzed as a function of melittin concentration at each temperature point at the increment of 2 °C, and the data were fit to a logistic function (Figure 2A). The T_{misc} shifts from 28 to 31 °C in the 0 and 5 μM melittin concentration range. Shifts in T_{misc} due to an additive in the membrane such as peptides and other molecules have been observed previously.^{35,36} It has been noted that, as a general rule, T_{misc} is elevated if an additive has a strong preference to one phase over the other.³⁷

To visualize the localization preference of melittin, C-terminal cysteine-modified melittin was labeled with Alexa Fluor 488 via a thiol-maleimide coupling reaction (melittin-AF488) and added to GUV1 where it induced phase separation. Melittin-AF488 strongly partitions to the L_d region with TR (Figure 2B,C). This result is consistent with a previous study where melittin labeled with NBD was also found to localize into the L_d region in similar GUVs composed of 0.2:0.6:0.2 DOPC/DPPC/Chol.²⁹ In that study, it was suggested that the selectivity originates from different compressibility moduli of the two phases: Because the DOPC-rich L_d phase is expected to be more compressible than the DPPC-rich L_o phase, L_d would be better able to accommodate the surface expansion associated with melittin binding. Together, these results show in addition to the well-known permeabilization and lysis effects, membrane-bound

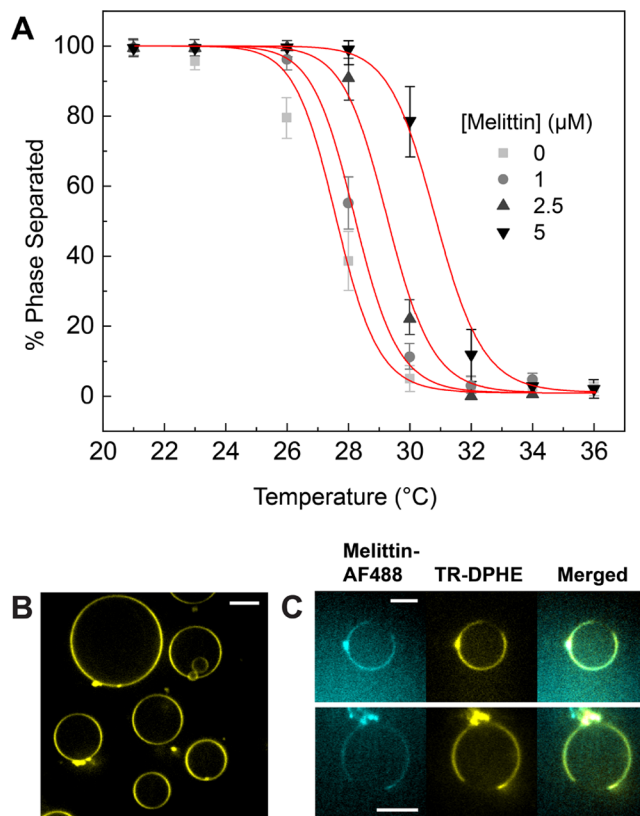


Figure 2. (A) The temperature dependence of phase separation on GUV2 incubated with melittin, measured in 2 °C increments. T_{misc} is elevated in a melittin-concentration-dependent manner. Approximately 100 GUVs were analyzed for each data point at room temperature, 21 °C. (B) GUV1 at room temperature before the addition of melittin. Scale bar = 5 μm . (C) Melittin-AF488 localizes to the L_d domain with TR. Scale bar 10 μm .

melittin can induce a global redistribution of lipids at a given temperature by shifting the miscibility equilibria.

PLA₂ and Melittin Synergistically Facilitate Phase Separation and Lysis. PLA₂ has been shown to induce lysis³⁸ and budding³⁹ in GUVs of various compositions. In our experiments, however, it showed minimal interaction and lytic or other effects on GUV1 over the experimental time window of 60 min and up to a 100 nM enzyme concentration (Figure 3A). In the presence of melittin, however, the PLA₂ activity is markedly enhanced. When 1 μM melittin is added to GUV1, PLA₂ induces further phase separation and rupturing in the nanomolar concentration range, with a majority population (~80%) of GUVs being ruptured at 100 nM (Figure 3B). This lytic efficiency exceeds that of 10 μM melittin alone, where ~70% of the same GUVs are ruptured. These results suggest that a synergistic effect exists between melittin and PLA₂, as small amounts of melittin and PLA₂ are minimally active in GUVs individually but have strong action in membrane lipid phase separation and lysis of the vesicles when both are present.

PLA₂ Localizes to the Boundary of Phase Separation. Given the significantly higher PLA₂ activity on phase separated GUVs, stronger interactions between PLA₂ and membranes were expected. To see where PLA₂ localized on phase separated GUVs, PLA₂ labeled with Alexa Fluor 647 via the *N*-hydroxysuccinimide-ester coupling reaction (PLA₂-AF647) was added to GUVs. Two types of phase separated GUVs were

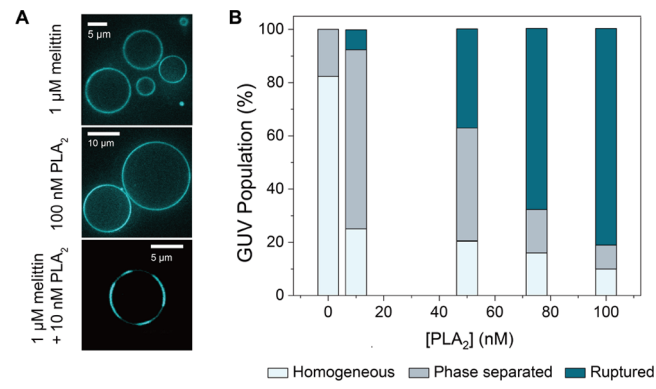
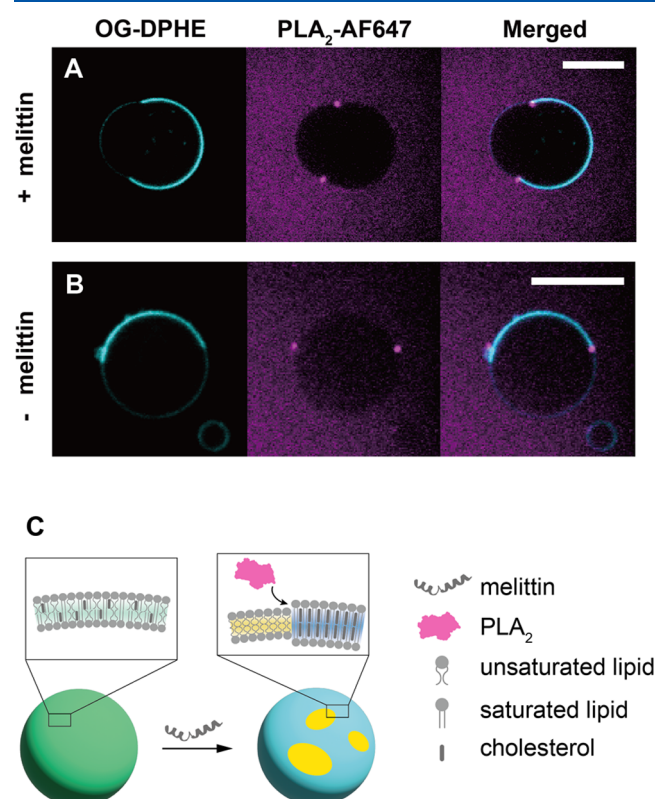


Figure 3. (A) At 1 μM melittin, the majority of GUV1 are homogeneous (top). PLA₂ shows little lytic activity over the experimental concentration range of up to 100 nM PLA₂ and time window of 60 min (middle). When the two are together, lipid phase separation is observed (bottom). (B) The population of GUV1 vesicles, incubated with melittin at 1 μM for 10 min, that are homogeneous, phase separated, and ruptured due to incubation with PLA₂ at various concentrations.

prepared: GUV1 with 1 μM melittin (Figure 4A) and GUV2, which is naturally phase separated at room temperature (Figure 4B). Where PLA₂-AF647 could be found on the vesicles, it was imaged at the boundary of phase separation, but not on the other areas of GUV surfaces (Figure 4A,B).



It is well documented that phase transition⁴⁰ as well as membrane defects and borders^{23,41} promote PLA₂ activation, and hydrolysis occurs predominantly at the domain boundaries.^{42,43} The reaction site of phospholipids is buried deep in an intact lipid bilayer.^{44,45} Atomic force microscopy and X-ray diffraction studies measured a height difference of 5–10 Å between the L_o and L_d regions in the membranes similar compositions,^{46,47} providing a defect in the membrane surface where PLA₂ may latch onto.³⁸ An important consequence is that once securely bound to the membrane at a defect PLA₂ becomes processive, catalyzing successive reactions without falling off the membrane. This results in a significantly longer dwell times, at membrane defects as observed by single-molecule tracking.²³ The observations presented here of PLA₂ exclusively localized at the phase separation boundaries of the vesicles are consistent with these previous findings.

PLA₂ Activity Promotes the Membrane Binding of Melittin. The observation that PLA₂ localizes to the boundaries of phase separation offers an explanation of how it becomes activated but not why it promotes further lipid phase separation and lysis. Given the catalytic potential, PLA₂ likely facilitates phase separation through lipid hydrolysis rather than as an additive that shifts equilibrium, which is the case for melittin. Based on the literature, we considered two possible mechanisms: (1) selective lipid hydrolysis by PLA₂ altering the lipid composition and (2) PLA₂ activity inducing melittin binding to membranes.

If the lipid hydrolysis is selective for one type of lipid over the other and is preferentially removed, then it could change the lipid composition such that T_{misc} is shifted. This has been demonstrated on the double-supported membrane islands, where PLA₂ was shown to degrade islands of L_d-like composition while L_o-like islands resisted hydrolysis.⁴¹ It was proposed that this selectivity originates from cholesterol blocking the access of PLA₂ to phospholipids. The inhibition of PLA₂ access to lipid substrate could occur via a competitive hydrogen bonding between the *sn*-2 carbonyl oxygen of the phospholipid and carboxyl group of cholesterol found in molecular dynamics simulations.⁴⁸ In the membrane islands with coexisting phases, the overall effect was the decrease of the cholesterol-deficient L_d region and increase in the cholesterol-rich L_o region. In GUVs with melittin, the overall effect of the selective hydrolysis could be a further phase separation and then lysis. Since the L_d region is thinner than the L_o region by 5–10 Å, the hydrolysis site of phospholipids in the L_d domain would be even more buried, disfavoring the selective hydrolysis in that region. Nevertheless, dynamic structural fluctuations may still allow PLA₂ to access the *sn*-2 acyl bond hydrolysis sites.

An alternative mechanism for PLA₂ promoting lipid phase separation and lysis is through the enhanced membrane recruitment of melittin. A previous work has shown that melittin binding to membrane measured by linear dichroism is increased when PLA₂ is present.⁴⁹ PLA₂ hydrolysis leaves lysophosphatidylcholine (lyso-PC) as a product, which changes the material properties of the membrane such as flexibility and porosity. In general, a more flexible membrane better accommodates melittin, and a previous work found a linear relation between the compressibility modulus and the lytic effect of melittin.⁵⁰ In that work, the inclusion of lyso-PC in egg-phosphatidylcholine (egg-PC) vesicles significantly increased the melittin activity, measured by vesicle leakage. In the present case, even though the PLA₂ itself is confined at

the boundary of membrane phase separation, lyso-PC can be expected to diffuse freely leading to this change in the membrane.

A significant distinction between the two mechanisms by which PLA₂ induces phase separation and lysis is that the second mechanism requires the presence of melittin in solution, whereas the first mechanism does not. Since selective hydrolysis is independent of melittin, enhanced phase separation and lysis should be evident for PLA₂ activated on phase separated GUVs without melittin if it is the major driving mechanism. Figure 5A illustrates the impact of melittin

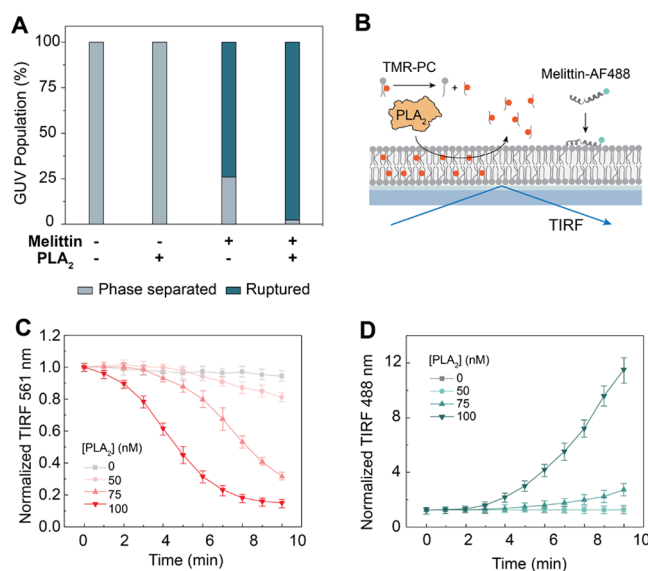


Figure 5. (A) The effect of melittin and PLA₂ on phase separated GUVs (GUV2), individually and in combination. The concentrations were 5 μM for melittin and 100 nM for PLA₂. (B) PLA₂-dependent melittin binding to the membrane was determined by TIRF on supported lipid bilayers containing 0.04% TMR-PC. At $t = 0$, PLA₂ and 200 nM melittin-AF488 were added together to SLBs. (C) PLA₂ catalytic activity was measured by the hydrolysis of TMR-PC on SLBs. (D) Membrane binding of melittin-AF488 was measured simultaneously with PLA₂ activity in (C).

and PLA₂ on GUV2, which are phase separated at room temperature without melittin. When administered alone, 100 nM PLA₂ does not induce lysis, although it is observed to localize at the boundaries of the phase separation (Figure 4B). This implies that despite PLA₂ being recruited to the membrane and catalyzing phospholipid hydrolysis in a processive manner, it is insufficient to cause vesicle lysis under the specified experimental conditions. However, with the addition of 5 μM melittin, a majority of the population undergoes rupture, and together with PLA₂, nearly all vesicles rupture. This observation suggests that PLA₂-induced lipid phase separation and lysis require the presence of melittin, indicating that selective hydrolysis likely plays a minor role, if any.

To see whether PLA₂ activity induces enhanced melittin binding to the membrane, we conducted experiments using planar supported lipid bilayers (SLBs) as illustrated in Figure 5B. These SLBs consisted of 89.96% DOPC, 10% DOPS, and 0.04% TopFluor TMR phosphocholine (TMR-PC). TMR-PC is a phospholipid labeled with a fluorophore in the *sn*-2 fatty acid chain and serves as an indicator as its hydrolysis by PLA₂ results in its release from the membrane. This property allowed

PLA₂ enzymatic activity to be measured through the time-dependent loss of fluorescence in total internal reflection fluorescence (TIRF) microscopy (Figure 5C). Concurrently, the membrane binding of melittin-AF488 was monitored by using TIRF (Figure 5D). The results of PLA₂ concentration-dependent measurements revealed that melittin exhibited a greater affinity for the membrane in a PLA₂-dependent manner. Although this experiment utilized solid-supported bilayers rather than freestanding membranes like GUVs, the findings provide supporting evidence that changes induced in the membrane by PLA₂ action facilitate increased melittin incorporation. This mechanism also aligns with the observation that PLA₂-mediated membrane lipid phase separation and lysis necessitate the presence of melittin.

CONCLUSIONS

In summary, our study reveals a synergistic lytic effect between melittin and PLA₂ mediated by a liquid–liquid miscibility phase transition in the GUV model membranes. Initially, melittin's binding to the membrane induces a lipid phase transition, altering the phase equilibrium and elevating the miscibility transition temperature. This leads to membrane lipid phase separation, creating a membrane discontinuity due to the thickness difference between the L_d and L_o regions. Subsequently, PLA₂ localizes to the phase boundaries and becomes active. Its activity propels further phase separation and vesicle lysis.

Two plausible mechanisms explain PLA₂'s role in driving phase separation and lysis. First, a preferential hydrolysis of unsaturated lipids in the L_d region removes these lipids, shifting the membrane composition toward enhanced phase separation and efficient vesicle lysis. Alternatively, PLA₂'s catalysis chemically and physically alters the membrane, leading to an increased incorporation of melittin and a greater degree of phase separation and lysis. Although both mechanisms may occur, the dependence of the observed synergism on melittin suggests that the second mechanism is likely the predominant driver with the first possibly playing a complementary role.

In essence, our findings underscore a positive feedback loop between melittin and PLA₂, contributing to the toxin's efficacy. This study illuminates a scenario where a biochemical substance actively manipulates and exploits the heterogeneity of membrane lipid distributions. Future investigations should explore the impact of melittin and PLA₂ on live cells, specifically examining whether they promote cellular membrane disruption through the spatial redistribution of lipids.

MATERIALS AND METHODS

Materials. The main components of the vesicles, such as phospholipids and cholesterol, were purchased from Avanti Polar Lipids (Alabaster, AL). These include: 1,2-dioleoyl-sn-glycero-3-phosphocholine (DOPC) (Cat. No. 850375), 1,2-dioleoyl-sn-glycero-3-phospho-L-serine (sodium salt) (DOPS) (Cat. No. 840035), 1,2-dipalmitoyl-sn-glycero-3-phosphocholine (DPPC) (Cat. No. 850355), cholesterol (Cat. No. 700100), and 1-oleoyl-2-(6-((4,4-difluoro-1,3-dimethyl-5-(4-methoxyphenyl)-4-bora-3a,4a-diaza-s-indacene-2-propionyl)amino)hexanoyl)-sn-glycero-3-phosphocholine (TopFluor TMR PC) (Cat. No. 810180). Fluorescently labeled lipids, Texas Red 1,2-dihexadecanoyl-sn-glycero-3-phosphoethanolamine (TR-DHPE) (Cat. No. T1395MP) and Oregon Green 488 1,2-dihexadecanoyl-sn-glycero-3-phosphoethanolamine (OG-DHPE) (Cat. No. O12650), were purchased from Thermo Fisher Scientific Inc. (Waltham, MA).

Synthesized bee venom melittin (Cat. No. RP10290) and custom cysteine-modified melittin were purchased from GenScript Biotech Corporation (Piscataway, NJ). Secretory phospholipase A₂ (Cat. No. S01779612), also derived from bee venom, was purchased from Fisher Scientific Co (Houston, TX). Alexa Fluor 488 C₅ maleimide (Cat. No. A10254) for labeling cysteine-modified melittin were purchased from Thermo Fisher Scientific Inc. (Waltham, MA). Alexa Fluor 647 (AF647) NHS ester (Cat. No. A20006) was used to label PLA₂. To facilitate 1:1 stoichiometric labeling, the enzyme and dye were reacted in a 1:0.8 stoichiometric ratio. The activity of AF-647 labeled PLA₂ was confirmed to be same as unmodified PLA₂ using EnzChek Phospholipase A₂ Assay Kit (ThermoFisher Cat. No. E10217).

Preparation of Giant Unilamellar Vesicles and Supported Lipid Bilayers. GUVs based on the ternary composition capable of undergoing liquid–liquid phase separation were prepared.² The two GUV compositions used here were of DOPC, DOPS, DPPC, cholesterol, TR-DHPE, and OG-DHPE at mole percentages of 39.8, 10, 20, 30, 0.1, and 0.1 for GUV1 and 29.8, 10, 40, 20, 0.1, and 0.1 for GUV2, respectively. GUV1 and GUV2 compositions without TR-DHPE were also made to observe PLA₂-AF647 addition to phase separated membranes (as the TR signal bleeds to the Cy5 channel). GUVs were prepared by electroformation using the standard protocol⁵¹ with the following modifications. The lipid mixtures of the desired compositions were prepared in chloroform. A quantity of 45.5 mmol of lipid mixtures in chloroform was spread on ITO-coated glass slides, dried under a vacuum, and assembled into a capacitor using a rubber spacer and conductive copper tape in 250 mM sucrose in water. GUVs generation from the lipid membrane was induced by passing an alternating current electric field (10.000 Hz, 5 V) provided by a waveform generator, for 3 h at 37 °C. The resulting vesicles were diluted in PBS (pH 7.4) and were allowed to sink to the surface of bovine serum albumin (BSA)-passivated (Sigma-Aldrich Cat. No. 05470) coverslips in microfluidic chambers made using Ibidi sticky-Slide VI 0.4 (Cat. No. 80608). For the experiments with PLA₂, 5 mM CaCl₂ was included. The vesicles were allowed to incubate for 5 min before imaging with spinning disc confocal microscopy. At least 100 GUVs were imaged for each population measurement.

Formation of supported lipid bilayers (SLBs) followed a previously established protocol.⁵² Briefly, SLBs were formed by the fusion of small unilamellar vesicles, prepared by extrusion through 30 nm pore membranes, on glass substrates cleaned by piranha etch (5 min in 3:1 H₂SO₄:H₂O₂). The bilayers were prepared in sticky-slide VI 0.4 microfluidic chambers assembled with the glass slide substrate for imaging. The integrity and fluidity of the bilayers and membrane-bound proteins was confirmed by fluorescence recovery after photobleaching (FRAP). All experiments were performed at room temperature, 21 °C.

Confocal and TIRF Microscopy. GUVs were visualized by spinning disk confocal microscopy, and the confocal scanner unit (CSU-X1-FW) produced by Yokogawa Electric Corporation (Tokyo, Japan) was used with a Nikon Ti2 Eclipse inverted fluorescence microscope (Tokyo, Japan). Temperature control was achieved using the Ibidi Temperature Controller (Gräfelfing, Germany). Images were taken in two fluorescence channels, TR and eGFP (for OG), to capture both the L_d and L_o phases. PLA₂ labeled with Alexa Fluor 647 was also imaged in the Cy5 channel. Temperature control was provided by an Ibidi Heating System (Cat. No. 12110). TIRF images for the SLB experiments were acquired on the same microscope with a 100× 1.49 NA oil immersion TIRF objective and an iXon EMCCD camera (Andor Technology, South Windsor, CT). Illumination sources for the confocal and TIRF microscopy were 488, 561, and 639 nm diode lasers (Vortan Laser Technology, Roseville, CA).

Data Analysis. Fluorescence images were loaded and processed using Fiji,⁵³ where fluorescence images of TR-DHPE and OG-DHPE were combined into a single composite image for determining phase separation. GUVs were counted as phase separated if there was demixing of the phases, observed by preferential fluorescence of TR-DHPE or OG-DHPE depending on the location in GUVs and if both phases were present on the given GUV, in compositions with both

dyes present. GUVs were counted if the center could be resolved without fluorescence.

AUTHOR INFORMATION

Corresponding Author

Jean K. Chung – Department of Chemistry, Colorado State University, Fort Collins, Colorado 80523, United States;  orcid.org/0000-0001-8221-0500; Email: jkchung@colostate.edu

Authors

Sein Min – Department of Chemistry, Colorado State University, Fort Collins, Colorado 80523, United States; Present Address: Seoul Women's University, Seoul, South Korea

Cyrus Picou – Department of Chemistry, Colorado State University, Fort Collins, Colorado 80523, United States;  orcid.org/0000-0002-3567-6428

Hyun Jin Jeong – Department of Chemistry, Colorado State University, Fort Collins, Colorado 80523, United States

Adam Bower – Department of Chemistry, Colorado State University, Fort Collins, Colorado 80523, United States; Present Address: Texas A&M University, College Station, Texas, United States

Keunhong Jeong – Department of Chemistry, Colorado State University, Fort Collins, Colorado 80523, United States; Present Address: Korea Military Academy, Seoul, South Korea;  orcid.org/0000-0003-1485-7235

Complete contact information is available at:

<https://pubs.acs.org/10.1021/acs.langmuir.3c03920>

Author Contributions

S.M. and C.P. contributed equally to this work. The authors confirm contribution to the paper as follows: study conception and design: J.K.C.; data collection: S.M., C.P.J., H.J.J., A.B.; data analysis: S.M., C.P.J., H.J.J.; interpretation of results: K.H.J., J.K.C.; draft manuscript preparation: C.P.J., J.K.C. All authors reviewed the results and approved the final version of the manuscript.

Funding

This work was supported by the National Science Foundation CAREER Award to JKC (MCB-2238109). H.J.J. was supported by Basic Science Research Program through the National Research Foundation of Korea, the Ministry of Education (NRF-2021R1A6A3A14046029).

Notes

The authors declare no competing financial interest.

ACKNOWLEDGMENTS

The authors thank Tyler Jepson for the initial experiments and Professor Il-Hyung "Eli" Lee at Montclair State University for helpful discussions.

REFERENCES

- (1) Singer, S. J.; Nicolson, G. L. The fluid mosaic model of the structure of cell membranes. *Science* **1972**, *175* (4023), 720–731.
- (2) Veatch, S. L.; Keller, S. L. Separation of Liquid Phases in Giant Vesicles of Ternary Mixtures of Phospholipids and Cholesterol. *Biophys. J.* **2003**, *85* (5), 3074–3083.
- (3) Shaw, T. R.; Ghosh, S.; Veatch, S. L. Critical Phenomena in Plasma Membrane Organization and Function. *Annu. Rev. Phys. Chem.* **2021**, *72*, 51–72.
- (4) Veatch, S. L.; Cicuta, P.; Sengupta, P.; Honerkamp-Smith, A.; Holowka, D.; Baird, B. Critical fluctuations in plasma membrane vesicles. *ACS Chem. Biol.* **2008**, *3* (5), 287–293.
- (5) Chung, J. K.; Huang, W. Y. C.; Carbone, C. B.; Nocka, L. M.; Parikh, A. N.; Vale, R. D.; Groves, J. T. Coupled membrane lipid miscibility and phosphotyrosine-driven protein condensation phase transitions. *Biophys. J.* **2021**, *120* (7), 1257–1265.
- (6) Shelby, S. A.; Castello-Serrano, I.; Wisser, K. C.; Levental, I.; Veatch, S. L. Membrane phase separation drives responsive assembly of receptor signaling domains. *Nat. Chem. Biol.* **2023**, *19* (6), 750–758.
- (7) Ureña, J.; Knight, A.; Lee, I. H. Membrane Cargo Density-Dependent Interaction between Protein and Lipid Domains on the Giant Unilamellar Vesicles. *Langmuir* **2022**, *38* (15), 4702–4712.
- (8) Wang, H. Y.; Chan, S. H.; Dey, S.; Castello-Serrano, I.; Rosen, M. K.; Ditlev, J. A.; Levental, K. R.; Levental, I. Coupling of protein condensates to ordered lipid domains determines functional membrane organization. *Sci. Adv.* **2023**, *9* (17), ead6205.
- (9) Dempsey, C. E. The actions of melittin on membranes. *Biochimica et Biophysica Acta (BBA) - Reviews on Biomembranes* **1990**, *1031* (2), 143–161.
- (10) Raghuraman, H.; Chattopadhyay, A. Melittin: a Membrane-active Peptide with Diverse Functions. *Bioscience Reports* **2007**, *27* (4–5), 189–223.
- (11) Klocek, G.; Schulthess, T.; Shai, Y.; Seelig, J. Thermodynamics of melittin binding to lipid bilayers. Aggregation and pore formation. *Biochemistry* **2009**, *48* (12), 2586–2596.
- (12) van den Bogaart, G.; Guzman, J. V.; Mika, J. T.; Poolman, B. On the Mechanism of Pore Formation by Melittin. *J. Biol. Chem.* **2008**, *283* (49), 33854–33857.
- (13) Miyazaki, Y.; Okazaki, S.; Shinoda, W. Free Energy Analysis of Membrane Pore Formation Process in the Presence of Multiple Melittin Peptides. *Biochimica et Biophysica Acta (BBA) - Biomembranes* **2019**, *1861* (7), 1409–1419.
- (14) Pino-Angeles, A.; Lazaridis, T. Effects of peptide charge, orientation, and concentration on melittin transmembrane pores. *Biophys. J.* **2018**, *114*, 2865.
- (15) Papo, N.; Shai, Y. Exploring Peptide Membrane Interaction Using Surface Plasmon Resonance: Differentiation between Pore Formation versus Membrane Disruption by Lytic Peptides†. *Biochemistry* **2003**, *42* (2), 458–466.
- (16) van den Bogaart, G.; Mika, J. T.; Krasnikov, V.; Poolman, B. The Lipid Dependence of Melittin Action Investigated by Dual-Color Fluorescence Burst Analysis. *Biophys. J.* **2007**, *93* (1), 154–163.
- (17) Ownby, C. L.; Powell, J. R.; Jiang, M.-S.; Fletcher, J. E. Melittin and phospholipase A2 from bee (*Apis mellifera*) venom cause necrosis of murine skeletal muscle in vivo. *Toxicon* **1997**, *35* (1), 67–80.
- (18) Lara Bitar, D. J.; Rima, M.; Al-Alam, J.; Sabatier, J.-M.; Fajloun, Z. Bee Venom PLA2 versus Snake Venom PLA2: Evaluation of Structural and Functional Properties. *Venoms and Toxins* **2021**, *1*, e01012021189841.
- (19) Yaacoub, C.; Rifi, M.; El-Obeid, D.; Mawlawi, H.; Sabatier, J.-M.; Coutard, B.; Fajloun, Z. The Cytotoxic Effect of *Apis mellifera* Venom with a Synergistic Potential of Its Two Main Components—Melittin and PLA2—On Colon Cancer HCT116 Cell Lines. *Molecules* **2021**, *26* (8), 2264.
- (20) Mollay, C.; Kreil, G. Enhancement of bee venom phospholipase A2 activity by melittin, direct lytic factor from cobra venom and polymyxin B. *FEBS Lett.* **1974**, *46* (1–2), 141–144.
- (21) Koumanov, K.; Momchilova, A.; Wolf, C. Bimodal regulatory effect of melittin and phospholipase A2-activating protein on human type II secretory phospholipase A2. *Cell Biol. Int.* **2003**, *27* (10), 871–877.
- (22) Yunes, R.; Goldhammer, A. R.; Garner, W. K.; Cordes, E. H. Phospholipases: Melittin facilitation of bee venom phospholipase A2-catalyzed hydrolysis of unsonicated lecithin liposomes. *Arch. Biochem. Biophys.* **1977**, *183* (1), 105–112.

(23) Jepson, T. A.; Hall, S. C.; Chung, J. K. Single-molecule phospholipase A2 becomes processive on melittin-induced membrane deformations. *Biophys. J.* **2022**, *121* (8), 1417–1423.

(24) Grandbois, M.; Clausen-Schaumann, H.; Gaub, H. Atomic force microscope imaging of phospholipid bilayer degradation by phospholipase A2. *Biophys. J.* **1998**, *74* (5), 2398–2404.

(25) Ray, S.; Scott, J. L.; Tatulian, S. A. Effects of lipid phase transition and membrane surface charge on the interfacial activation of phospholipase A2. *Biochemistry* **2007**, *46* (45), 13089–13100.

(26) Veatch, S. L.; Keller, S. L. Organization in lipid membranes containing cholesterol. *Phys. Rev. Lett.* **2002**, *89* (26), 268101.

(27) Vahey, M. D.; Fletcher, D. A. The biology of boundary conditions: cellular reconstitution in one, two, and three dimensions. *Curr. Opin. Cell Biol.* **2014**, *26*, 60–68.

(28) Strömstedt, A. A.; Wessman, P.; Ringstad, L.; Edwards, K.; Malmsten, M. Effect of lipid headgroup composition on the interaction between melittin and lipid bilayers. *J. Colloid Interface Sci.* **2007**, *311* (1), 59–69.

(29) Yu, Y.; Vroman, J. A.; Bae, S. C.; Granick, S. Vesicle Budding Induced by a Pore-Forming Peptide. *J. Am. Chem. Soc.* **2010**, *132* (1), 195–201.

(30) Himeno, H.; Shimokawa, N.; Komura, S.; Andelman, D.; Hamada, T.; Takagi, M. Charge-induced phase separation in lipid membranes. *Soft Matter* **2014**, *10* (40), 7959–7967.

(31) Shimokawa, N.; Hamada, T. Physical Concept to Explain the Regulation of Lipid Membrane Phase Separation under Isothermal Conditions. *Life* **2023**, *13* (5), 1105.

(32) Vequi-Suplicy, C. C.; Riske, K. A.; Knorr, R. L.; Dimova, R. Vesicles with charged domains. *Biochimica et Biophysica Acta (BBA) - Biomembranes* **2010**, *1798* (7), 1338–1347.

(33) Blosser, M. C.; Starr, J. B.; Turtle, C. W.; Ashcraft, J.; Keller, S. L. Minimal Effect of Lipid Charge on Membrane Miscibility Phase Behavior in Three Ternary Systems. *Biophys. J.* **2013**, *104* (12), 2629–2638.

(34) Liu, A. P.; Fletcher, D. A. Actin polymerization serves as a membrane domain switch in model lipid bilayers. *Biophys. J.* **2006**, *91* (11), 4064–4070.

(35) Bacia, K.; Schuette, C. G.; Kahya, N.; Jahn, R.; Schwille, P. SNAREs prefer liquid-disordered over "raft" (liquid-ordered) domains when reconstituted into giant unilamellar vesicles. *J. Biol. Chem.* **2004**, *279* (36), 37951–37955.

(36) Doeven, M. K.; Folgering, J. H.; Krasnikov, V.; Geertsma, E. R.; van den Bogaart, G.; Poolman, B. Distribution, lateral mobility and function of membrane proteins incorporated into giant unilamellar vesicles. *Biophys. J.* **2005**, *88* (2), 1134–1142.

(37) Ferguson, F. D.; Jones, T. K. *The Phase Rule*; Butterworths, 1996.

(38) Zhang, P.; Villanueva, V.; Kalkowski, J.; Liu, C.; Pham, T.; Perez-Salas, U.; Bu, W.; Lin, B.; Liu, Y. Polyunsaturated Phospholipid Modified Membrane Degradation Catalyzed by a Secreted Phospholipase A2. *Langmuir* **2019**, *35* (36), 11643–11650.

(39) Staneva, G.; Angelova, M. I.; Koumanov, K. Phospholipase A2 promotes raft budding and fission from giant liposomes. *Chem. Phys. Lipids* **2004**, *129* (1), 53–62.

(40) Mouritsen, O. G.; Andresen, T. L.; Halperin, A.; Hansen, P. L.; Jakobsen, A. F.; Jensen, U. B.; Jensen, M. Ø.; Jørgensen, K.; Kaasgaard, T.; Leidy, C.; et al. Activation of interfacial enzymes at membrane surfaces. *J. Phys.: Condens. Matter* **2006**, *18* (28), S1293.

(41) Simonsen, A. C. Activation of Phospholipase A2 by Ternary Model Membranes. *Biophys. J.* **2008**, *94* (10), 3966–3975.

(42) Gudmand, M.; Rocha, S.; Hatzakis, N. S.; Peneva, K.; Müllen, K.; Stamou, D.; Uji-I, H.; Hofkens, J.; Bjørnholm, T.; Heimburg, T. Influence of lipid heterogeneity and phase behavior on phospholipase A2 action at the single molecule level. *Biophys. J.* **2010**, *98* (9), 1873–1882.

(43) Chiu, C. R.; Huang, W. N.; Wu, W. G.; Yang, T. S. Fluorescence single-molecule study of cobra phospholipase A2 action on a supported gel-phase lipid bilayer. *ChemPhysChem* **2009**, *10* (3), 549–558.

(44) Kučerka, N.; Tristram-Nagle, S.; Nagle, J. F. Structure of Fully Hydrated Fluid Phase Lipid Bilayers with Monounsaturated Chains. *J. Membr. Biol.* **2006**, *208* (3), 193–202.

(45) Kyrychenko, A.; Ladokhin, A. S. Molecular Dynamics Simulations of Depth Distribution of Spin-Labeled Phospholipids within Lipid Bilayer. *J. Phys. Chem. B* **2013**, *117* (19), 5875–5885.

(46) Jensen, M. H.; Morris, E. J.; Simonsen, A. C. Domain shapes, coarsening, and random patterns in ternary membranes. *Langmuir* **2007**, *23* (15), 8135–8141.

(47) Chen, L.; Yu, Z.; Quinn, P. J. The partition of cholesterol between ordered and fluid bilayers of phosphatidylcholine: a synchrotron X-ray diffraction study. *Biochim. Biophys. Acta* **2007**, *1768* (11), 2873–2881.

(48) Smondyrev, A. M.; Berkowitz, M. L. Structure of Dipalmitoylphosphatidylcholine/Cholesterol Bilayer at Low and High Cholesterol Concentrations: Molecular Dynamics Simulation. *Biophys. J.* **1999**, *77* (4), 2075–2089.

(49) Damianoglou, A.; Rodger, A.; Pridmore, C.; Dafforn, T. R.; Mosely, J. A.; Sanderson, J. M.; Hicks, M. R. The synergistic action of melittin and phospholipase A2 with lipid membranes: development of linear dichroism for membrane-insertion kinetics. *Protein Pept. Lett.* **2010**, *17* (11), 1351–1362.

(50) Allende, D.; Simon, S. A.; McIntosh, T. J. Melittin-induced bilayer leakage depends on lipid material properties: evidence for toroidal pores. *Biophys. J.* **2005**, *88* (3), 1828–1837.

(51) Schmid, E. M.; Richmond, D. L.; Fletcher, D. A. Reconstitution of proteins on electroformed giant unilamellar vesicles. *Methods Cell Biol.* **2015**, *128*, 319–338.

(52) Lin, W. C.; Yu, C. H.; Triffo, S.; Groves, J. T. Supported membrane formation, characterization, functionalization, and patterning for application in biological science and technology. *Curr. Protoc. Chem. Biol.* **2010**, *2* (4), 235–269.

(53) Schindelin, J.; Arganda-Carreras, I.; Frise, E.; Kaynig, V.; Longair, M.; Pietzsch, T.; Preibisch, S.; Rueden, C.; Saalfeld, S.; Schmid, B.; et al. Fiji: an open-source platform for biological-image analysis. *Nat. Methods* **2012**, *9* (7), 676–682.